Biophys. Struct. Mechanism 3, 275–289 (1977)

Biophysics of Structure and Mechanism

An Error in Interpretation of Double-Reciprocal Plots and Scatchard Plots in Studies of Binding of Fluorescent Probes to Proteins, and Alternative Proposals for Determining Binding Parameters

Kenneth Zierler

Departments of Physiology and Medicine, The Johns Hopkins University School of Medicine, 725 North Wolfe Street, Baltimore, Maryland 21205, USA

Abstract. One of the objects of experiments in which a fluorochrome is added to suspensions of cell membranes is to determine the parameters n and K_D, the capacity of unit mass of protein to bind fluorochrome and the dissociation constant, respectively. Currently, these are estimated from Scatchard plots, construction of which first requires that observed fluorescence intensity be converted to moles of bound fluorochrome. This in turn is said to be possible by analysis of the intercept of a plot of reciprocal fluorescence intensity against reciprocal protein concentration. However, analysis of the classical mass action equilibrium equation, upon which the foregoing procedures are said to be based, reveals that the intercept of the double-reciprocal plot always underestimates the desired value. The error is formalized and shown to increase without bound with fluorochrome concentration. The error in turn leads to erroneous assessment of n and K_D. Alternative methods for calculating the desired parameters are proposed, based on direct plots of fluorescence intensity.

Key words: Binding – Fluorescent probes – Membrane protein – Scatchard plots.

In the course of studying binding of the fluorescent probe, 8-anilino-1-naphthalene-sulfonic acid (ANS), to suspensions of sarcolemmal vesicles we plotted the reciprocal of the intensity of fluorescence of membrane-bound ANS against the reciprocal of the protein concentration of the suspension, at constant total ANS concentration. The relationship was always linear, with regression coefficients usually > 0.99 and never < 0.98.

The intercept of the best fitted line upon the reciprocal intensity axis is interpreted as the reciprocal of the intensity of membrane-bound ANS at infinite membrane protein concentration; hence it is held to represent the intensity given by binding of all the ANS. This value for intensity of total ANS is then used in construction of Scatchard plots from data in which, at constant membrane protein concentration, the concentration of ANS is varied.

It is not clear when this sort of procedure was first used, nor why, but it has been used for some time. Scatchard [1] in 1949, in his classic work on attractions of proteins for small molecules and ions, in which the equation is given for the plot that now bears his name, stated (p. 669): "Recent usage has been to invert the law of mass action solved for $\bar{\nu}$ to give

$$\frac{1}{\bar{\nu}} = \frac{1}{n} + \left(\frac{1}{kn}\right)\frac{1}{c},$$

to plot $1/\bar{\nu}$ against $1/c$, to draw the best straight line and call its intercept $1/n$ and its slope $1/kn$. This has the disadvantage of concealing deviations from ideal laws, and of attempting straight lines where there should be curvature". In Scatchard's notation, $\bar{\nu}$ is the average number of sites occupied by the small molecule or ion per molecule of protein, n is the maximum possible number of such sites available initially per molecule of protein, kn is the classical association constant for the equilibrium. c is not defined explicitly in Scatchard's paper, but it seems to be the concentration of unbound small molecule or ion. $\bar{\nu}$ can be considered also as the concentration of bound small molecule or ion per unit concentration of protein.

Earlier, Klotz [2], in 1946, used the expression

$$\frac{1}{r} = \frac{1}{n} + \frac{K}{n}\frac{1}{(A)},$$

where, in his notation, r is the concentration of bound ion per unit concentration of protein, K is the dissociation constant, and (A) is the concentration of unbound ion. Klotz's formulation can be rearranged to yield the relationship we use as springboard for analysis in this paper, Equation (4).

We were struck initially by two features. First, we found in the literature on binding of fluorescent probes no occasion in which the investigator exploited the information that must reside in the slope of the double-reciprocal plot (as used recently, not as described by Scatchard), nor any mention of the interpretation of that slope in terms of parameters of the system. Second, we could establish experimental conditions in which, reproducibly, we obtained intercepts significantly less than zero. Such intercepts cannot have the physical meaning attributed to the intercept, for there cannot be a negative total ANS concentration.

It seemed advisable to examine more fully the implications of the double-reciprocal plot.

We begin with recognition of the empirical relation,

$$1/I = a_0 + a_1(1/[Pr]), \tag{1}$$

where I is intensity of fluorescence of membrane-bound ANS, $[Pr]$ is concentration of membrane protein in the suspension, and a_0 and a_1 are empirical constants.

Implications in the literature are that Equation (1) derives from the classical equilibrium mass action equation,

$$(n - \bar{\nu})\,[Pr]\,[A]_F = K_D\bar{\nu}[Pr] = K_D[A]_B\,, \tag{2}$$

where $[A]$ is concentration of ANS or other small molecule or ion, subscripts F and B refer to free and bound fractions, respectively, $\bar{\nu}$ is the average number of ANS

molecules bound per unit mass of membrane protein, n is the total possible number of ANS binding sites per unit mass of membrane protein, and K_D is an equilibrium constant for dissociation. This formulation is equivalent to that given by Klotz [2] in 1946 in his assessment of multiple binding sites.

We will make use of the relationship, total $[A]$ is

$$[A] = [A]_F + [A]_B . \tag{3}$$

From Equations (2) and (3) we obtain the double-reciprocal form

$$\frac{1}{[A]_B} = \frac{1}{[A]} + \left(\frac{K_D}{[A]\,(n - \bar{v})}\right) \frac{1}{[Pr]} . \tag{4a}$$

An alternative form of Equation (4a) is

$$\frac{1}{[A]_B} = \frac{1}{[A]} + \left(\frac{K_D + [A]_F}{[A]\,n}\right) \frac{1}{[Pr]} . \tag{4b}$$

In both Equations (4), the modifier of $(1/[Pr])$ is not constant, but is explicit either in the variable $\bar{v}$ or in the variable $[A]_F$.

If the experimental range of fluorochrome concentration is constrained so that intensity of fluorescence is proportional to concentration, then

$$I = m[A]_B , \tag{5a}$$

where m is constant. For ANS, at least, owing to differences in quantum yield of 100-fold, fluorescence of $[A]_F$ is undetected in the presence of $[A]_B$.

When all the fluorochrome in the system is membrane-bound, there is maximum intensity of fluorescence,

$$I_\infty = m[A] . \tag{5b}$$

With Equation (5), Equation (4) is recast in terms of measured fluorescence intensity,

$$\frac{1}{I} = \frac{1}{I_\infty} + \left(\frac{K_D}{I_\infty(n - \bar{v})}\right) \frac{1}{[Pr]} . \tag{6}$$

It is the purpose of the double-reciprocal plot to obtain the intercept, purported to be $1/I_\infty$, as indicated in Equation (6). From this calculated value of I_∞ and the known value of $[A]$, the coefficient m is determined (Eq. 5b). From this value of m and the various values of I, the concentration of bound fluorochrome $[A]_B$, is determined (Eq. 5a).

Then, in experiments at constant $[Pr]$ and variable $[A]$, the Scatchard plot is drafted; $[A]_B/([A]_F[Pr])$ is plotted against $[A]_B/[Pr]$. The object of the Scatchard plot is determination of the parameters n and K_D. Rearrangement of Equation (2) gives the Scatchard formulation,

$$\frac{[A]_B/[Pr]}{[A]_F} = \frac{n}{K_D} - \frac{1}{K_D} [A]_B/[Pr] . \tag{7}$$

The slope is $-1/K_D$, the intercept on the X-axis is n, and the intercept on the Y-axis is n/K_D.

We now ask how well the double-reciprocal plot $1/I$ against $1/[Pr]$, yields an estimate of $1/I_\infty$.

Compare the empirical relationship (1) with Equation (6). It appears off-hand that the empirical constant a_0 is $1/I_\infty$, in keeping with the conventional interpretation of the intercept. But it also appears that the empirical constant a_1 is the expression in parentheses, modifying $1/[Pr]$ in Equation (6). But this expression is a function of $\bar{\nu}$ which is not a constant; $\bar{\nu}$ is an implicit function of I. Therefore, it cannot be true that the empirical intercept a_0 is identical to $1/I_\infty$. We will develop an analytical expression for the difference between a_0 and $1/I_\infty$, but first we will analyze the function $1/I$ of Equation (6).

The first derivative,

$$\frac{d(1/I)}{d(1/[Pr])} = \frac{nm^2K_D[Pr]^2}{I_\infty(mn[Pr] - I)^2 + mK_DI^2} \tag{8}$$

is always greater than zero. As $[Pr]$ grows large without bound, I increases toward I_∞, and the limit of the first derivative is $K_D/(nI_\infty)$, which, from Equation (6), is the limit expected for $\bar{\nu}$ negligible compared to n; that is, for very large protein concentration with relatively small initial concentration of A. Thus, the slope of the double-reciprocal plot is the conventional $K_D/(nI_\infty)$ only at the intercept on the $(1/I)$-axis, and exceeds that value for all other values of $1/[Pr]$. As $[Pr]$ grows small $1/[Pr]$ grows large and the slope approaches a constant, $(mK_D + I_\infty)/mnI_\infty$.

The second derivative is

$$\frac{d^2(1/I)}{d(1/[Pr])^2} = 2\,N[Pr]I(mn[Pr] - I)\,(I_\infty(mn[Pr] - I) - mK_DI)^2/D^3\,, \tag{9}$$

where N and D are the numerator and the denominator, respectively, on the right-hand side of Equation (8). Since all terms are greater than zero, the second derivative is always positive.

Hence, $(1/I)$ is a monotone, non-decreasing function of $(1/[Pr])$, concave upward. The best linear fit to such a curve must yield an intercept which falls below the true value of $(1/I)$ for zero $(1/[Pr])$; that is, the estimated intercept is less than $(1/I_\infty)$.

It is important to note that this error exists even if, empirically, the plot of (I/I_∞) against $(1/[Pr])$ fits a straight line excellently, with a regression coefficient close to unity. Real data cover only a finite range, a small segment of the set of possible values of $(1/[Pr])$. Excellent linear fits to small segments are possible. If the fit is good enough, the slope of that best linear fit must always be greater than (K_D/I_∞), since the slope equals (K_D/I_∞) only at infinite $[Pr]$. Hence, backward extrapolation of this line to intersect the $(1/I)$ axis must always yield an intercept less than $(1/I_\infty)$. The closer the values of $(1/[Pr])$ are to zero, the better the intercept estimates $1/I_\infty$.

These points are illustrated in Figures 1 and 2, which were constructed as follows:

From the classical equilibrium mass action Equation (2), with the substitution of I/m for $[A]_B$ (Eq. 5a) and $(I_\infty - I)/m$ for $[A]_F$,

$$I = \tfrac{1}{2}(b - \sqrt{R}), \tag{10}$$

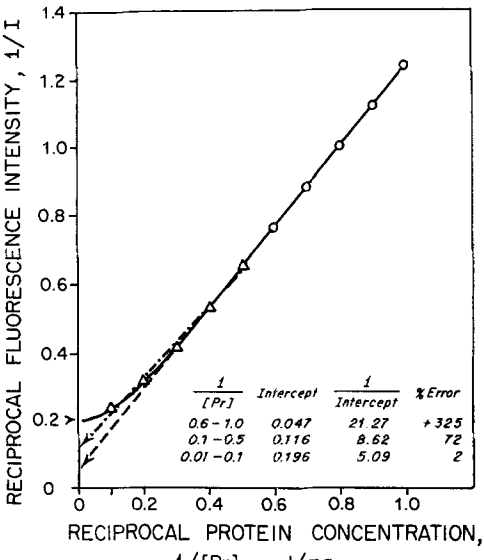

Fig. 1

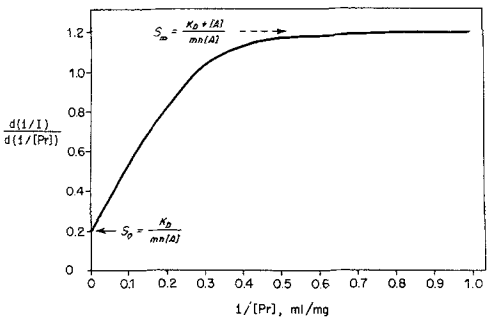

Fig. 2

Fig. 1. Double-reciprocal plot, $1/I$ against $1/[Pr]$, generated from classical equilibrium mass action equation with the parameters set as follows: $m = 1$ fluorescence intensity unit per nmole of fluorochrome, $n = 1$ nmole fluorochrome per mg protein, $K_D = 10^{-6}$ M. Fluorochrome concentration $[A] = 5 \times 10^{-6}$ M. Protein concentration varied independently from 1—100 mg/ml. The curve is non-linear in its entirety. The true intercept on the $1/I$ axis is 0.2. Linear extrapolation of any portion of the curve underestimates the intercept. Linear extrapolation from data indicated by circles (the uppermost points) yields the lowest intercept (bottom arrow), although the regression coefficient is 1 (to 5 decimal places). Linear extrapolation from data indicated by triangles (the intermediate points) leads to the intermediate intercept. Linear extrapolation of the lowest points (and most curved portion) intercepts at the highest arrow, although still below the true intercept. The errors of the intercept are, respectively 325, 72, and 2%

Fig. 2. The slope of the double-reciprocal plot against $1/[Pr]$, generated from the same data used to construct Figure 1. The slope is not constant, contrary to expectations from its current use. It approaches a constant and maximum at high values of $1/[Pr]$. As $1/[Pr]$ tends to zero the slope tends to become a linear function of $1/[Pr]$; that is, the second derivative of $1/I$ with respect to $1/[Pr]$ tends to become constant, and the slope is maximum at zero $1/[Pr]$. See text for analysis

where $b = mn[Pr] + mK_{D+I_\infty}$, and $R = b^2 - 4\ mnI_\infty[Pr]$. Values for the parameters m, n, and K_D were set. Then a value for $[A] = I_\infty/m$ was selected, and a family of values for I was determined over a range of the independent variable, $[Pr]$.

Figure 1 illustrates the results applied to a double-reciprocal plot, $1/I$ against $1/[Pr]$, over a 100-fold range of values for $[Pr]$. Over the range from $0.6 \leq [Pr] \leq 1$ ml/mg (the open circles in Fig. 1), the relationship is exquisitely linear (regression coefficients > 0.999), but extrapolation to the $1/I$ axis intercepts at 0.047 (the lower broken line in Fig. 1), well below the true value of $1/I_\infty$, 0.2. The error yields a 325% over-estimate of I_∞. [Not shown in Figure 1 are results of extension over the range $1.0 \leq 1/[Pr] \leq 10$, $(0.1 \leq [Pr] \leq 1$ mg/ml). The linear relationship continued over this range, with an intercept at 0.0368, yielding a 440% over-estimate of I_∞]. Over

the range from $0.1 \leq 1/[Pr] \leq 0.5$ ml/mg (the triangles in Fig. 1), the relationship becomes curved, concave upward. The linear regression still gives a reasonably good fit ($r = 0.997$), but the intercept (the upper broken line in Fig. 1) is still less than the true intercept, and I_∞ is over-estimated by 72%. Over the range $0.01 \leq 1/[Pr] \leq 0.1$ ml/mg ($10 \leq [Pr] \leq 100$ mg/ml) the double-reciprocal plot has greater curvature. It is in fact headed toward the true intercept, 0.2, but linear regression analysis ($r = 0.992$) still yields a falsely low intercept, although the error is small; I_∞ is over-estimated by only 2%.

Figure 1, of course, is only illustrative, although, no matter what values of m, n, and K_D are selected, for any given value of $[A]$ the double-reciprocal plot will always have the shape illustrated in Figure 1 if it is examined over a sufficiently wide range of protein concentration. Over a range of values of $[Pr]$ sufficiently small, the double-reciprocal plot will always overestimate I_∞. Indeed when $[A]$ is selected sufficiently large compared to $n[Pr]$ the intercept becomes less than zero, giving an absurd answer to the estimate of I_∞. On the other hand, as $n[Pr]$ grows large compared to $[A]$, the intercept obtained by linear regression analysis of the double-reciprocal plot approaches the true value of $1/I_\infty$.

There may, of course, be practical problems with working with the very large concentrations of protein that may be required in any given circumstance to obtain an acceptable estimate of $1/I_\infty$ from the double-reciprocal plot. In a later section of this analysis we shall consider alternative approaches.

Figure 2 is a plot of the slopes of the curve shown in Figure 1 against reciprocal protein concentration; that is, it is a plot of the left-hand member of Equation (8) against $1/[Pr]$. The function rises nearly linearly from some positive value at zero $1/[Pr]$, is monotone concave downward, and continues toward a plateau at high $1/[Pr]$. The region of plateau (= constant slope) corresponds to the linear region of the double-reciprocal plot. As we shall see later, this constant slope, S_∞ in Figure 2, is always $(K_D + [A])/(mn[A])$. The initial value of the function, S_0 in Figure 2, at zero $1/[Pr]$ is always $K_D/(mn[A])$.

Notice that K_D can be calculated from the two slopes, S_0 and S_∞. The equations for the slopes are a pair of simultaneous equations in K_D and mn. Their solution yields $K_D = S_0[A]/(S_\infty - S_0)$. This is not likely to be a useful method for obtaining K_D since it requires measurement over two ranges of values of $[Pr]$. More useful solutions are given later.

Clearly, as conditions become such that S_0 and S_∞ approach one another, the double-reciprocal plot tends to become linear over its entirety. From the equations for these two limiting slopes, it is evident that the slope of the double-reciprocal plot tends to become constant as $K_D \to (K_D + [A])$, that is, as $[A]$ tends to become negligible compared to K_D. For example, for $K_D = 60 \times 10^{-6}$ M, at $[A] = 10^{-6}$ M the double-reciprocal plot is nearly linear over its entire length. In this condition the intercept of the linear extrapolation of the double-reciprocal plot is within 2% of the correct intercept.

However, it is emphasized that linearity of the double-reciprocal plot is not of itself an adequate test of the validity of the extrapolated intercept because, as illustrated in Figure 1, no matter what the relation between K_D and $[A]$, the double-reciprocal plot becomes linear as $1/[Pr]$ grows large. Thus, there is a broad range of

values for $[Pr]$ over which the dobule-reciprocal plot is linear, and from which linear extrapolation to the intercept gives an unbounded error of estimate of I_∞.

We turn now to obtain an analytic expression for the error of the estimate of I_∞ from the intercept of a double-reciprocal plot.

Designate the linear function obtained empirically, previously defined in Equation (1), by the new function

$$Y = a_0 + a_1([Pr]),$$

to distinguish it from the true function $(1/I)$, defined in Equation (6). We seek an expression for $(1/I_\infty) - a_0$.

The sum of squares of the differences between Y and $(1/I)$, over the range from $1/[Pr] = \alpha$ to $1/[Pr] = \beta$, is

$$\int_\alpha^\beta (Y - (1/I))^2 \, d(1/[Pr]).$$

Conventionally, the constants a_0 and a_1 are determined by differentiating this integral with respect to a_0 and, separately, with respect to a_1, setting the two derivatives each equal to zero, to obtain the minimum sum, and solving the pair of simultaneous linear equations.

The result is that

$$a_0 = f(\alpha, \beta)\left\{2(\beta^2 - \alpha^2)\int_\alpha^\beta \frac{1}{I}\, d\left(\frac{1}{[Pr]}\right) - 3(\beta^3 - \alpha^3)\int_\alpha^\beta \frac{1}{I[Pr]}\, d\left(\frac{1}{[Pr]}\right)\right\}, \tag{11}$$

where

$$f(\alpha, \beta) = 2(\beta - \alpha)/(4(\beta^2 - \alpha^2) - 3(\beta^2 - \alpha\beta + \alpha^2)).$$

If the total binding capacity of the system, $n[Pr]$, is very large compared to the initial concentration of ANS, or other bindable molecule, then I is always equal to or nearly equal to I_∞, and $a_0 = 1/I_\infty$. For all other cases $a_0 < 1/I_\infty$.

The error of the estimate is

$$\varepsilon = (1/I_\infty) - a_0, \tag{12}$$

where a_0 is given in Equation (11).

a_0 is a function of the limits α and β, over which $1/[Pr]$ is permitted to range experimentally, and a function of $1/I$. Since I is an implicit function of m, n, and K_D, these parameters must also influence the magnitude of the error. The influence of these parameters can be estimated by re-writing Equation (12) explicitly in these parameters and then differentiating partially with respect to each of them. Of more interest are those variables over which the investigator exerts control, $[A]$ and $[Pr]$.

It is evident from inspection of Equation (11), for a_0, and from Figure 1 that the closer the observed points are to the $1/I$ axis the smaller the error of estimate of the intercept. Hence, the larger $[Pr]$ and the smaller $[A]$, the less the error. The critical requirement is that $\bar{\nu}/n$, the fraction of association sites actually occupied, must remain nearly zero over the range of values of $[Pr]$ at the given $[A]$. Achievement of this condition may be practical under some circumstances and impractical under others. It may be impractical if such small values of $[A]$ are required that the instrumental sensing system is unreliable, or if such larges values of $[Pr]$ are required that

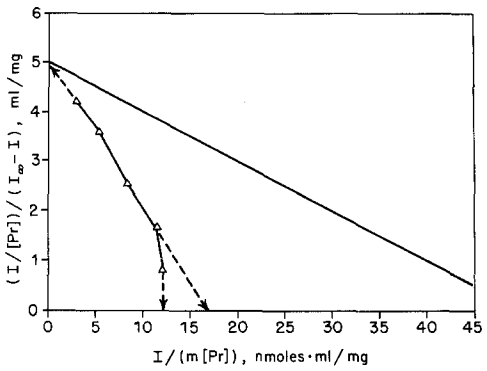

Fig. 3. Influence on the Scatchard plot of the error of intercept of double-reciprocal plots. See text for details. Parameters: $m = 30$ intensity units per nmole fluorochrome, $n =$ 50 nmoles per mg protein, $K_D = 10^{-5}$ M, $[Pr]$ $= 0.1$ mg/ml, $1 \leq [A] \leq 64 \times 10^{-6}$ M. The straight line was constructed by use of the correct parameters. The heavy curve was constructed by use of the erroneous estimates of m, each point (Δ) calculated on the basis of the individual erroneous m derived from a double-reciprocal plot at the corresponding value of $[A]$. See text for analysis

undesirable effects occur, such as extensive light scattering in the case of protein.

Before we consider alternative possibilities for estimation of m, n, and K_D, let us look into the effects of the error on the construction of Scatchard plots.

Figure 3 illustrates a Scatchard plot constructed on the basis of the erroneous estimates of I_∞ and of m. A family of double-reciprocal plots were constructed from simulated data, using Equation (10), $I = (b - \sqrt{R})/2$, assumed values for m, n, and K_D. $[A]$ was varied from 1–64 μM, and the range of $[Pr]$ was selected to yield a reasonably long segment of the "linear" portion of the double-reciprocal plot (see Fig. 1). As $[A]$ increased, the over-estimate of I_∞ and of m grew larger. From the sets of data for I as a function of $[Pr]$ at constant $[A]$ a single value of $[Pr]$ was selected, and I was made a function of $[A]$ at constant $[Pr]$.

The Scatchard plot is, in the notation of this communication, a plot of $(I/[Pr])/(I_\infty - I)$ against $(I/m)/[Pr]$, where $(I/m)/[Pr] = \bar{\nu}$, and $(I/[Pr])/(I_\infty - I) = \bar{\nu}/[A]_F$. From the double-reciprocal plot I_∞ was taken as $1/a_0$ and m as $1/(a_0[A])$. In Figure 3 the Scatchard plot constructed from the estimates of a_0 and the erroneous estimate of m is non-linear, compared to the linear plot made from correct values for I_∞ and m. The two plots are headed toward the same intercept on the Y-axis, yielding similar estimates of that intercept, n/K_D. However, they are headed toward quite different intercepts on the X-axis. The correct X-axis intercept is n. In the illustration, n is 50. The erroneous data, as plotted, are headed toward an apparent intercept at 12, giving estimates of n and K_D that are only about 25% of the correct values. An investigator confronted with data plotted as the curve in Figure 3 might be tempted to suggest that something was wrong with the lowest datum, and, ignoring that point he might draw a straight line through only the first four points. These data do fit a straight line reasonably well. Such a line in this illustration extrapolates to intercept the X-axis at a value about one-third of the value of the correct intercept. The slope of that line is about three times the correct slope. Since the true slope equals $-1/K_D$, the false slope gives a value only one third the true value. Not plotted in this illustration are data at higher values of $[A]$. For those values of $[A]$ the estimate of m was so falsely high that I did not grow as rapidly as m, and $(I/[Pr])/m$ actually decreased as $[A]$ increased. Thus the curve bent back upon itself and moved toward the Y-axis as $[A]$ increased.

Faced with a curve of the kind illustrated in Figure 3 the investigator might be tempted to suppose that the Scatchard plot suggests cooperativity, and he might construct a Hill plot, the logarithm of the ratio of the bound to free binding sites against the logarithm of free ligand. If he did, he would find the slope greater than unity, and he might be tempted to conclude that there was cooperativity.

The classical equilibrium mass action Equation (2) can be rearranged to give the concentration of bound fluorochrome, $[A]_B$, as an explicit function of the two independent variables, the ligand $[Pr]$ and the total fluorochrome $[A]$. The solution is a quadratic:

$$[A]_B = \tfrac{1}{2}\{(n[Pr] + K_D + [A]) - ((n[Pr] + K_D + [A])^2 - 4n[A][Pr])^{1/2}\}. \quad (13)$$

As was pointed out with reference to Equation (10), the coordinate solution, which is the sum of the two terms on the right-hand side of Equation (13), is inadmissible, owing to the restriction that $[A]_B \leq [A]$.

We also defined the linear relation between fluorescence intensity and concentration of bound fluorochrome,

$$I = m[A]_B. \quad (14)$$

Thus the solution for fluorescence intensity, I, from Equations (13) and (14) is a function of two independent variables, $[Pr]$ and $[A]$, and of three parameters, m, n, and K_D. The object of experiment is realization of the parameters n and K_D, and this cannot be accomplished unless m is also known.

Customarily we carry out two types of experiments. In one $[A]$ is held constant and $[Pr]$ is the sole independent variable. In the other $[Pr]$ is held constant and $[A]$ is the sole independent variable. Hence, I becomes a function of either the variable $[Pr]$ or the variable $[A]$. Plots of these two functions of I, computed with the aid of Equations (13) and (14) are illustrated for the full range of the appropriate independent variable in Figures 4 and 5.

In both cases, I rises to a maximum where it remains independent of further increases with independent variable. In both cases the limiting value of I is useful.

For I as a function of $[Pr]$ at constant $[A]$,

$$\lim_{[Pr] \to \infty} I([Pr]) \equiv I_\infty = m[A], \quad (15)$$

whence the value of the parameter m becomes known.

For I as a function of $[A]$ at constant $[Pr]$,

$$\lim_{[A] \to \infty} I([A]) = mn[Pr], \quad (16)$$

whence the value of the product of parameters, mn, becomes known.

Combination of the two types of experiments yields the value of the parameter n.

With m and n computed, with $[A]$ and $[Pr]$ set by the investigator, and with I determined by fluorimetry, K_D can then be computed from the mass action equation, rearranged for explicit solution:

$$K_D = \frac{n[Pr]([A] - [A]_B)}{[A]_B} - [A]. \quad (17)$$

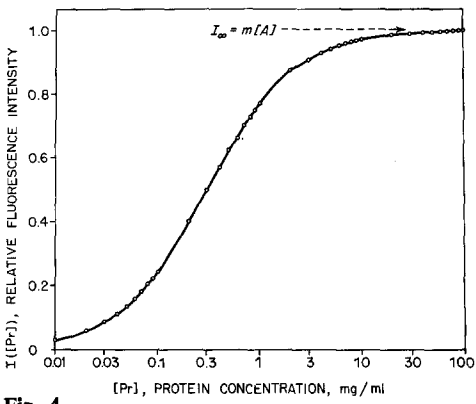

Fig. 4

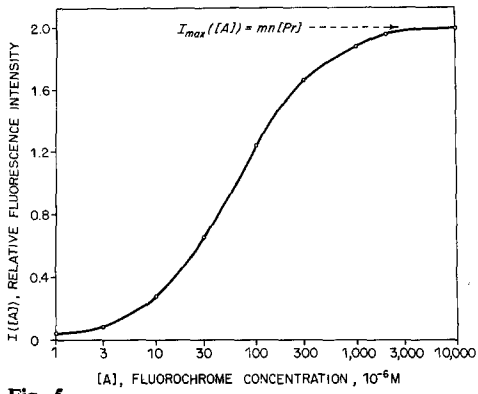

Fig. 5

Fig. 4. Relative fluorescence intensity as a function of protein concentration, $[Pr]$, at constant fluorochrome concentration. $[Pr]$ is plotted on a logarithmic scale in order to display the full range of values of $[Pr]$. $I([Pr])$ was generated from the equilibrium mass action equation. Parameters were: $m = 1$ intensity unit per nmole fluorochrome, $n = 200$ nmoles fluorochrome per mg protein, $K_D = 60 \times 10^{-6}$ M. The parameters were selected to correspond to those reported for a system of ANS and mitochondrial membrane by Azzi et al. [3]. Fluorochrome concentration: $[A] = 10^{-6}$ M. Notice the high protein concentration required to achieve plateau, at which all fluorochrome is bound. At plateau $I([Pr]) = I_\infty = m[A]$, from which m is calculated. Note that a plot of I against $[Pr]$, rather than against log $[Pr]$, does not have a flexure; the second derivative is always negative

Fig. 5. Relative fluorescence intensity as a function of fluorochrome concentration at constant protein concentration, $[Pr] = 0.1$ mg/ml. Fluorochrome concentration plotted on a logarithmic scale to display the full range of values of $[A]$. Notice the extraordinarily high values of $[A]$ required to saturate the protein. When it is saturated, maximum $I[A] = mn[Pr]$. Note also that a plot of I against $[A]$ rather than against log $[A]$, does not have a flexure

The computation can be checked by carrying it out at several values of $I([Pr])$ and of $I([A])$.

It is worth emphasizing here that if it is not possible to carry out experiments incorporating a range of independent variables that gives plateau values of I, there is no point in constructing a double-reciprocal plot, $1/I$ against $1/[Pr]$, because the extrapolated intercept of the double-reciprocal plot gives the correct value of $1/I_\infty$, hence of m, only when plateau values of $I([Pr])$ have been attained. The direct plot of I against $[Pr]$ has the advantage of letting the investigator see whether I has indeed reached its maximum, hence that the experiments have been conducted over the intended useful range. There is no such internal check in the case of the double-reciprocal plots.

Figures 4 and 5 were constructed from data for n and K_D reported by Azzi et al. [3]. In this case, attainment of plateau values of $I([Pr])$ requires a much larger concentration of Pr than it is generally practical to use in such experiments, and attainment of plateau values of $I([A])$ requires larger concentrations of A than practical.

There are circumstances in which experiments cannot be conducted at sufficiently high concentrations of $[A]$ or of $[Pr]$ to obtain the desired maximum values of $I([A])$ and $I([Pr])$. In this case the investigator may be able to exploit certain properties of the system in which at constant $[A]$ useful information is obtained as $[Pr] \to 0$ and at constant $[Pr]$ as $[A] \to 0$. This useful information lies in the derivatives of the function $I([A])$ and $I([Pr])$.

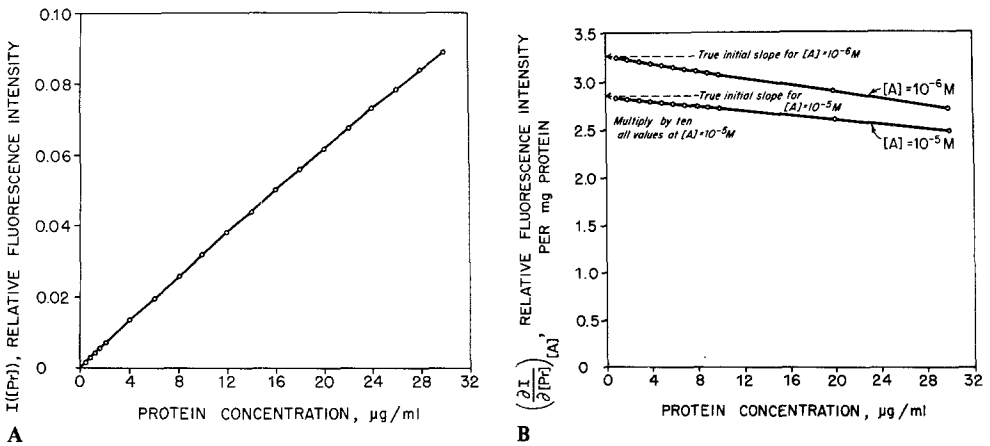

Fig. 6A. Relative fluorescence intensity as a function of protein concentration, at low protein concentration. Same parameters as in Figure 4. Note that, unlike Figure 4, $[Pr]$ is plotted on a linear scale and $[Pr]$ is in units μg/ml, rather than mg/ml. Over this range of $[Pr]$, the function is nearly linear. The best linear fit to the whole body of data plotted from $1 \leq [Pr] \leq 30$ μg/ml has a slope not substantially different from the true initial slope

Fig. 6B. Slope of fluorescence intensity, $(\partial I/\partial[Pr])_{[A]}$, at constant $[A]$, against $[Pr]$. Data are from those for $I([Pr])$ at 10^{-6} M $[A]$, illustrated in Figure 4, and for 10^{-5} M $[A]$. Data are true derivatives [see text Equation (18)]. True initial slopes $S_{[A]}$, indicated by arrows on vertical axis. Note that scale for $\partial I/\partial[Pr]$ with $[A] = 10^{-5}$ M must be multiplied by 10. Values of initial slopes and $[A]$'s are inserted into Equation (26) and solved for K_D. In this case the solution is $K_D = 59.8 \times 10^{-6}$ M. Actual value of K_D used in construction of Figures 4 and 5 was 60×10^{-6} M

In experiments in which $[A]$ is constant and $[Pr]$ is varied, the slope of the plot of I against $[Pr]$ is the partial derivative of I with respect to $[Pr]$, which from Equations (13) and (14) is

$$\left(\frac{\partial I}{\partial [Pr]}\right)_{[A]} = \frac{mn}{2}\left\{1 - \frac{n[Pr] + K_D - [A]}{((n[Pr] + K_D + [A])^2 - 4\,n[Pr][A]^{1/2}}\right\}. \tag{18}$$

We investigate this slope as we let $[Pr]$ tend to zero. With terms in $[Pr]$ removed from Equation (18),

$$\underset{[Pr]\to 0}{\text{limit}} \left(\frac{\partial I}{\partial [Pr]}\right)_{[A]} = \frac{mn[A]}{K_D + [A]} \equiv S_{[A]}\,. \tag{19}$$

Figure 6 illustrates the function $(\partial I/\partial[Pr])_{[A]}$ over the full range of $[Pr]$. The curve was computed from Equation (18), using the data for $I([Pr])$ illustrated in Figure 4. The initial slope has the numerical value $mn[A]/(K_D + [A])$. It contains the unknown parameters K_D and the product mn.

Designate this initial slope $S_{[A]}$.

We now conduct experiments in which $[Pr]$ is constant and $[A]$ is the independent variable. The partial derivative of I with respect to $[A]$, from Equations (13) and (14) is

$$\left(\frac{\partial I}{\partial [A]}\right)_{[Pr]} = \frac{m}{2}\left\{1 - \frac{[A] + K_D - n[Pr]}{((([A] + K_D + n[Pr])^2 - 4\,n[Pr][A])^{1/2}}\right\}. \tag{20}$$

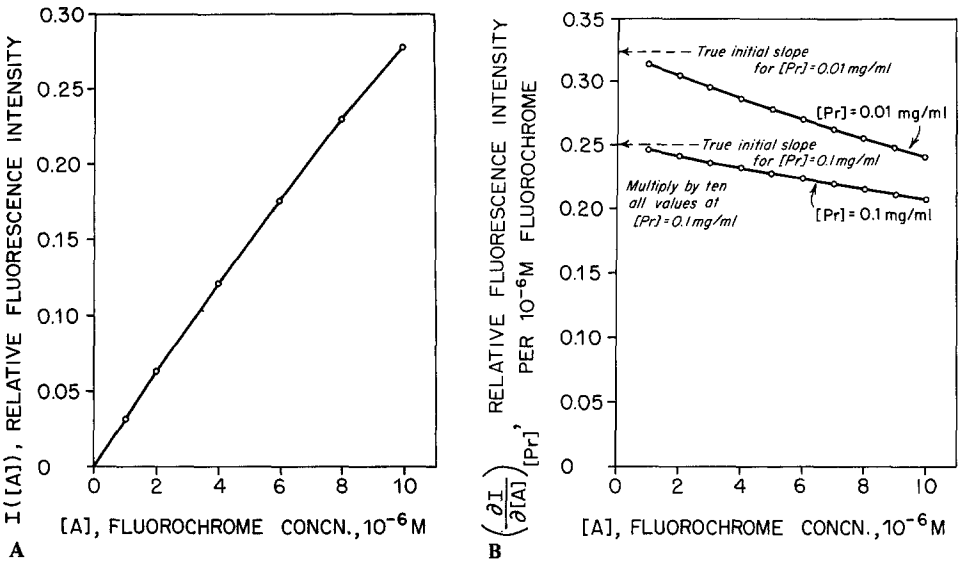

Fig. 7A. Relative fluorescence intensity as a function of fluorochrome concentration, at low fluorochrome concentrations. Same parameters as in Figure 5. The best linear fit to the whole body of data in this figure has a slope not substantially different from the true initial slope.

Fig. 7B. Slope of fluorescence intensity $(\partial I/\partial [A])_{[Pr]}$, at constant $[Pr]$, against $[A]$. Data are those for $I([A])$ at 0.01 mg/ml $[Pr]$, illustrated in Figure 5, and at 0.1 mg/ml $[Pr]$. Data are true derivatives [see Equation (20)]. True initial slope indicated by arrows on vertical axis. Note that scale for $\partial I/\partial [A]$ with $[Pr] = 0.1$ mg/ml must be multiplied by 10. Values of initial slope, $S_{[Pr]}$, together with those for $S_{[A]}$, $[A]$, and the solution for K_D, from Figure 6B, are inserted into Equation (27) and solved for n. In this case the solution is $n = 199.3$ nmoles/mg protein. Actual value of n used in construction of Figures 4 and 5 was 200 nmoles/mg

As $[A]$ tends to zero, terms in $[A]$ tend to disappear and

$$\lim_{[A] \to 0} \left(\frac{\partial I}{\partial [A]}\right)_{[Pr]} = \frac{mn[Pr]}{K_D + n[Pr]} \equiv S_{[Pr]} . \tag{21}$$

Figure 7 illustrate the function $(\partial I/\partial [A])_{[Pr]}$ over the full range of $[A]$ computed from Equation (20) and the data for $I([A])$ plotted previously in Figure 5. The initial slope, which we designate $S_{[Pr]}$, has the numerical value of $mn[Pr]/(K_D + n[Pr])$. It contains the unknown parameters K_D, n, and the product mn.

Suppose we carry out two experiments at constant $[A]$ and at varying $[Pr]$. In one of these $[A] = [A]_1$; in the other $[A] = [A]_2$ we also carry out two experiments at constant $[Pr]$ and at varying $[A]$. In one $[Pr] = [Pr]_1$; in the other $[Pr] = [Pr]_2$. From these we generate four equations of the type of Equations (19) and (21):

$$S_{[A]1} = mn[A]_1/(K_D + [A]_1) \tag{22}$$

$$S_{[A]2} = mn[A]_2/(K_D + [A]_2) \tag{23}$$

$$S_{[Pr]1} = mn[Pr]_1/(K_D + [Pr]_1) \tag{24}$$

$$S_{[Pr]2} = mn[Pr]_2/(K_D + [Pr]_2) \tag{25}$$

Thus we have four equations for the three unknown parameters, K_D m, and n. There is one redundant equation. We require only any three of the four equations for the solution. These three may be two at constant $[A]$, Equations (22) and (23) and one at constant $[Pr]$, either Equation (24) or (25), or either one at constant $[A]$ and two at constant $[Pr]$.

If we use the former set, from Equations (22), (23), and either (24), or (25),

$$K_D = \frac{S_{[A]2} - S_{[A]1}}{S_{[A]1}/[A]_1) - (S_{[A]2}/[A]_2)}, \tag{26}$$

and

$$n = \frac{S_{[A]1}}{S_{[Pr]}} + \frac{1}{S_{[Pr]}} \left(\frac{S_{[A]1}}{[A]_1} - \frac{S_{[Pr]}}{[Pr]} \right) K_D, \tag{27}$$

where absence of subscript notation means that either of the pair of equations may be used, as long as the same one is used throughout.

Note that n and K_D are determined without the need to determine m, contrary to methods presently in use. If it is desired to determine m, it is computed from any of Equations (22) through (25) by insertion of the numerical values for K_D and n.

If we use the set of equations at two values of $[Pr]$ and one at $[A]$, from Equations (22), (24), and (25),

$$K_D = \frac{[A][Pr]_1[Pr]_2 \, S_{[A]} (S_{[Pr]1} - S_{[Pr]2})}{[A] \, S_{[Pr]1} \, S_{[Pr]2} ([Pr]_1 - [Pr]_2) - [Pr]_1[Pr]_2 \, S_{[A]}(S_{[Pr]1} - S_{[Pr]2})}, \tag{28}$$

and

$$n = \frac{([Pr]_1 \, S_{[Pr]2} - [Pr]_2 \, S_{[Pr]1}) K_D}{[Pr]_1[Pr]_2 \, (S_{[Pr]1} - S_{[Pr]2})}. \tag{29}$$

As in the previous case, it is not necessary to solve for m to obtain K_D and n, but m can be computed if desired by insertion of the values for K_D and n into any of Equations (22) through (25).

Fortunately, practical estimates of the initial slopes are simple. Figures 6B and 7B show that the slopes decrease nearly linearly and slowly from initial values. Little error is made by use of real values near the intercept, which may be obtained by finite differences: $\Delta I([Pr])/\Delta[Pr]$, and $\Delta I([A])/\Delta[A]$, for small values of $[Pr]$ and $[A]$, respectively. Closer estimate is obtained by linear extrapolation of these finite differences to the intercept, indicated in Figures 6B and 7B. Note that each of these finite differences underestimates the true initial slope, but these errors tend to cancel out when one uses two sets of slopes, for example, for calculation of K_D illustrated in Figure 6B.

Finally, the initial slope can be estimated sufficiently well for practical purposes by conventional linear regression analysis of the plot of $I([Pr])$ and of $I([A])$. As illustrated in Figures 6A and 7A, these plots are nearly straight lines over a broad range of low concentrations of $[Pr]$ and of $[A]$, respectively. The slopes of these regression lines are acceptably close to the true initial slopes.

For those who prefer graphic solutions, the following is a graphic solution of one set of simultaneous linear equations. Consider the set of experiments for which Equations (22), (23), and (24) apply. Solve Equations (22) and (23) explicitly for K_D.

$$K_D = -[A]_1 + \frac{[A]_1}{S_{[A]1}} mn, \quad K_D = -[A]_2 + \frac{[A]_2}{S_{[A]2}} mn.$$

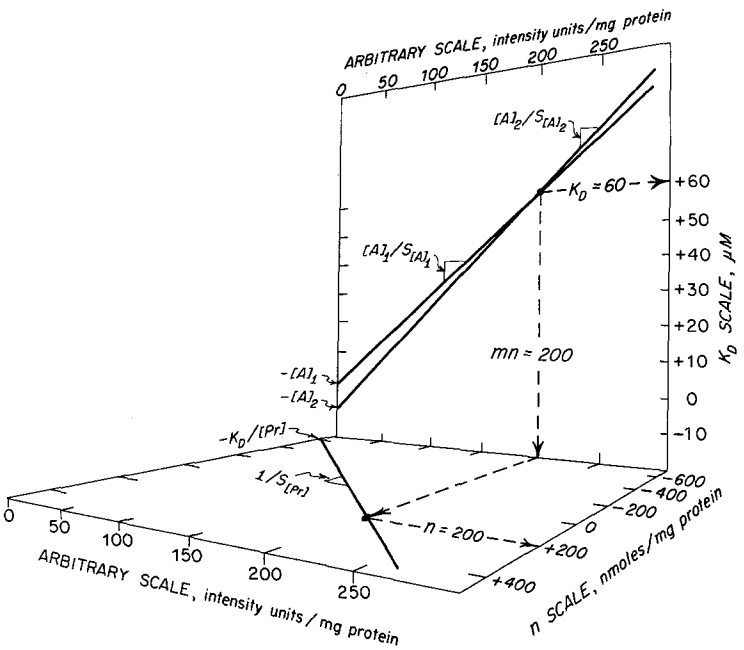

Fig. 8. Graphic determinations of parameters K_D, n, and mn. The vertical scale has dimensions of μM and is determined by the intercept $-[A]$. The slope of the line is $[A]/S_{[A]}$. Data from Figure 6 are used to construct two such lines. Their intersection is at K_D on the vertical axis and mn on the horizontal axis. The second plot, projected toward the reader perpendicular to the plane of the paper, adds a scale in dimensions of nmoles/mg protein, determined by the intercept $-K_D/[Pr]$, where K_D is the value yielded by the intersection above. The slope $1/S_{[Pr]}$ is from Figure 7. Intersection of this line with mn gives the value of n

Both K_D and mn are unknown. We wish to solve for K_D. A plot of K_D against any arbitrary variable, x, yields a straight line,

$$K_D = -[A] + ([A]/S_{[A]})\, x\,,$$

with intercept $-[A]$ and slope $[A]/S_{[A]}$. Both intercept and slope are known experimentally. Set one intercept at $-[A]_1$ and from it construct a line with slope $[A]_1/S_{[A]1}$. Set the other intercept at $-[A]_2$ and from it construct another line with slope $[A]_2/S_{[A]2}$. The intersection of the two lines gives the value of K_D.

Equation (24) solved explicitly for n is

$$n = -\frac{K_D}{[Pr]} + \frac{1}{S_{[Pr]}}\, mn\,.$$

Plot n on the vertical axis against the same arbitrary variable x, and on the same horizontal scale. The intercept on the n-axis is $-K_D/[Pr]$, which is known since K_D has been determined. From the intercept construct a line with slope $1/S_{[Pr]}$. The intersection of this line with the perpendicular from the X-axis at the point at which K_D was determined gives the value of n. The perpendicular itself intersects the X-axis at mn.

Note that the X-axis may be any arbitrary linear scale, and the K_D scale and n scale need have no predetermined relation to one another. Correctness of the K_D and n scales is achieved by placement of the intercepts.

The graphic solution is illustrated in Figure 8, based on the data displayed in Figures 6 and 7.

Summary

Investigators use fluorescent dye to investigate the capacity of a system to associate with the fluorochrome and the affinity of the system for dye. The parameters to be determined are n and K_D. It has been the custom to estimate numerical values of these parameters by means of Scatchard plots. To do so, however, it has been necessary first to relate fluorescence intensity to concentration of bound dye, through a coefficient designated m in this analysis. It has been the custom to estimate m from manipulations of calculations from a double-reciprocal plot $1/I$ against $1/[Pr]$. This method is based on an erroneous interpretation of the formal expression for the double-reciprocal plot. The error always over-estimates m, and the over-estimate can be unbounded. This error leads to curvature of the, now erroneous, Scatchard plot and to erroneous estimate of n and K_D.

It is shown that the desired parameters, n and K_D, can be obtained from direct plots of I against $[Pr]$ at constant concentration of fluorochrome, $[A]$, and of I against $[A]$ at constant $[Pr]$. Two types of limiting conditions are analyzed. In one the behavior of I is examined as $[Pr]$ and $[A]$ grow large. In the other the behavior of the slopes of the $I-[Pr]$ and $I-[A]$ plots are examined as $[Pr]$ and $[A]$ tend toward zero. Both of these extremes yield equations from which n and K_D can be computed. Hence, the investigator has a choice of conditions, election of which depends upon the experimental system.

Acknowledgements. This project was supported by NIH research grant number AM 17574, awarded by the National Institute of Arthritis, Metabolism and Digestive Diseases, PHS/DHEW, and by a grant from the Muscular Dystrophy Associations of America, Inc.

References

1. Scatchard, G.: The attraction of proteins for small molecules and ions. Ann. N.Y. Acad. Sci. **51**, 660–672 (1949)
2. Klotz, I. M.: The application of the law of mass action to binding by proteins. Interactions with calcium. Arch. Biochem. **9**, 109–117 (1946).
3. Azzi, A., Chance, B., Radda, G. K., Lee, C. P.: A fluorescence probe of energy-dependent structure changes in fragmented membranes. Biochemistry **62**, 612–619 (1969)

Received July 31, 1976/Accepted January 24, 1977